ONLINE FIRST April 13, 2026

Engineering Transactions, **74**, https://doi.org/10.24423/engtrans.2025.3626
Institute of Fundamental Technological Research Polish Academy of Sciences (IPPT PAN)
Université de Lorraine • Poznan University of Technology

Research Paper

Simulation Study of Direct-Shear Tests on FRP-to-Concrete Bonded Joints by Means of XFEM

Iwona Jankowiak

Poznan University of Technology
Poznań, Poland

e-mail: iwona.jankowiak@put.poznan.pl

A proper numerical modelling of FRP-to-concrete bonded joints is crucial for determining their strength. In this paper, the results of numerical analyses performed using XFEM on such joints in direct-shear test are presented. The study uses a fracture mechanics approach based on the traction-separation law to define the FRP-concrete interface. It includes the definition of damage initiation as well as damage evolution, taking advantage of the fracture energy of plain concrete as well as the interfacial fracture energy of the analysed joint. The interfacial fracture energy of the bonded joint is essential for accurately describing the local bond–slip behaviour. The numerical study aims to investigate the sensitivity of direct-shear test models to the magnitude of fracture energies, material strengths, the type of adhesive, and the length of FRP-to-concrete joint. Some general results and conclusions of the performed analyses are presented.

Keywords: FRP strengthening, XFEM analysis, modes of fracture energy, FRP-to-concrete joints, interfacial fracture energy, traction-separation law.

Notations

σ_n, τ_s	–	normal and shear bond strengths of the interface,
σ, τ	–	normal and shear stresses of the contact under mixed-mode loading,
G_{I}, G_{II}	–	fracture energy components of Modes I and II,
$G_{F\mathrm{I}}$, $G_{F\mathrm{II}}$	–	critical fracture energies under pure Modes I and II loading,
P	–	reaction force at the FRP-concrete interface in the direct-shear test on FRP-to-concrete bonded joints,
s	–	relative movement (slip) between the FRP and the concrete under shear stress in the direct-shear test of FRP-concrete bonded joints,
u	–	displacement at the end of the FRP strip due to the reaction force P in the direct shear-test,
L	–	lengths of the FRP-concrete joint,
G_{cr}	–	interfacial fracture energy; value equal to the value of fracture energy $G_{F\mathrm{II}}$ for Mode II,
ε_{11}	–	axial strain along the FRP-concrete joint.

1. Introduction

Externally bonded fibre-reinforced polymer (FRP) materials have been widely used for many years as an alternative method to traditional techniques for strengthening reinforced concrete (RC) structural members [1, 2]. The principles of application of this type of strengthening are well recognized and described in the literature [3, 4]. However, aspects related to the failure of FRP-strengthened concrete members are still a subject of research. They are mainly focused on the FRP strip debonding from the concrete surface. This debonding is initiated at the toe of flexural or flexural/shear cracks of concrete members (interfacial debonding, IC) and usually leads to a premature and brittle member failure [5, 6]. Therefore, to design RC beams against FRP debonding failures, proper modelling of the FRP-to-concrete interface is required, and the results obtained from direct-shear tests provide very valuable inputs in this regard.

There are many available results of laboratory tests performed on direct-shear FRP-concrete joints [7–10]. The tests consider the influence of the main parameters on the strength of the bonded joint, such as the length, width, and thickness of the FRP strip, its modulus of elasticity, and the shear span-to-depth ratio. They have been implemented in the development of design methods for RC beam strengthening [11, 12]. These results are also very useful for the validation of analytical and numerical models proposed in recent years. The analytical models, often simplified, presented in [7, 13, 14] are based on an assumed stress-slip relation between the FRP strip and concrete; they use elements of linear elastic fracture mechanics (LEFM), or cohesive crack model (CCM), as well as finite fracture mechanics (FFM). Different bond-slip models for FRP-to-concrete bonded joints have been proposed and presented, for example in [8]. They are based on different τ-slip relation and on interfacial fracture energy [7]. It was also pointed out that the type of adhesive layer (rigid or flexible) can influence the behaviour of FRP-to-concrete joint, mainly affecting the effective bond length and the bond strength itself [9].

The application of the finite element method (FEM) to the analysis of FRP-concrete joints has made it possible to create much more detailed models of the FRP-concrete interface. For example, in [6], the modelling of debonding failure in FRP-strengthened RC beams used the concept of a cohesive zone model, and for concrete cover separation, special cohesive elements were implemented.

Using the classical FEM, it is very difficult or impossible to address fracture mechanics problems, such as modelling material separation and fracture processes with realistic crack initiation and propagation, which is particularly valuable for concrete [16–19].

The extended finite element method (XFEM) allows to model cracks using discontinuous functions, such as the Heaviside step function, without the need

to explicitly mesh the crack itself; cracks can occur arbitrarily in the interior of finite elements. XFEM enables detailed analysis of cracks, material interfaces, and multiple crack interactions within a single model.

The strip debonding failure has been observed in laboratory tests on RC beam elements strengthened with FRP strips, performed and described extensively in [5]. In these experiments, the main goal was to recognise the overall response of strengthened concrete beams in terms of their load-carrying capacity and stiffness increase. The local effects, such as debonding and its impact on the behaviour of the entire system, were not considered at that time. The concrete damaged plasticity material model [5, 6, 15] was employed in the analyses, which allowed the ultimate load-carrying capacity to be estimated with sufficient accuracy. These results were then validated by laboratory tests. A very good agreement with the experimental results was observed. It was concluded that if only the ultimate load capacity estimation is required, XFEM does not need to be applied.

The present study is aimed at the detailed modelling of a direct-shear test, which is a highly discontinuous and nonlinear phenomenon. In the study, XFEM was applied. A parametric analysis of the main characteristics affecting the performance of these joints has been carried, and its results will be used for preparing the planned laboratory tests.

2. Application of XFEM for crack modelling of FRP-concrete bonded joints

The XFEM was first proposed in the context of fracture by Belytschko and Black [20], subsequently, the method was further developed [21, 22] and is still successfully used for the analysis of cracking phenomena in concrete elements. A comprehensive study of the fracture process in concrete and RC, by means of constitutive models formulated within continuum mechanics, where both continuous and discontinuous modelling approaches (using CCM and XFEM) were used, is presented in [23]. It has been proven that XFEM is an alternative method to FEM that extends the allowable basis functions, known as partition of unity methods [23, 24]. This method can be used not only to model cracks in homogenous material but also cracking occurring between two different materials (bimaterial interface cracks) [25]. Numerical modelling of crack propagation in plain concrete under Mode II and mixed-mode condition, with successful comparison with experiment results, was given in [26, 27].

When applied to crack propagation problems, XFEM introduces two extra sets of functions in addition to standard FEM nodal basis functions: a step function $H(x)$ to capture the discontinuity in displacement across a crack, and a set of functions $F_i(x)$, typically expressed in polar coordinates centred

at the crack tip, capturing stress singularity in that region. The extra basis functions are defined as the product of these enrichment functions and the standard nodal basis function to ensure that the basis functions remain mesh-based and local to the enriched nodes.

This method does not require the mesh to match the geometry of discontinuities. It can be used to simulate the initiation and propagation of a discrete crack by using a fracture energy criterion along an arbitrary, solution-dependent path in the bulk material, without the need for remeshing (crack propagation is not tied to element boundaries in the mesh) [23, 25].

In XFEM modelling of the FRP-concrete shear test, the failure mechanism, including degradation and eventual separation between the two surfaces, consists of two components: a damage initiation criterion and a damage evolution law.

Damage is initiated (either when an additional crack is introduced, or when the crack length of an existing crack is extended after an equilibrium increment), when the contact stresses and/or contact separations satisfy the damage initiation criterion, i.e., when the fracture criterion reaches a value of 1 within a given tolerance.

In 2D analysis concerning the phenomena of the direct-shear test of FRP strips from the concrete surface, the quadratic nominal stress criterion [15, 28] was assumed as the damage initiation criterion:

$$\left(\frac{\langle\sigma\rangle}{\sigma_n}\right)^2 + \left(\frac{\tau}{\tau_s}\right)^2 = 1, \tag{2.1}$$

where σ_n and τ_s are the normal and shear bond strengths of the interface, respectively; σ and τ are the normal and shear stresses at the interface under mixed-mode loading, respectively. The symbol $\langle\ \rangle$ is used to signify that purely compressive stress does not initiate damage, i.e., $\langle\sigma\rangle = 0$ if $\sigma < 0$ and $\langle\sigma\rangle = \sigma$ if $\sigma \geq 0$.

The damage evolution law defines the post damage-initiation material behaviour and describes the rate of degradation of the material stiffness once the initiation criterion has been reached. In the analysis of the direct-shear test of FRP strips from the concrete surface, the damage evolution is described using a linear softening model expressed in terms of fracture energy. The adopted power-law fracture energy criterion (with a power of 2) [15, 28, 29] is defined as a function of mode mix, using normal-mode fracture energy G_{I} (Mode I) for plain concrete and shear-mode fracture energy G_{II} (Mode II) for the interfacial FRP-concrete joint:

$$\left(\frac{G_{\mathrm{I}}}{G_{F\mathrm{I}}}\right)^2 + \left(\frac{G_{\mathrm{II}}}{G_{F\mathrm{II}}}\right)^2 = 1, \tag{2.2}$$

where G_{I} and G_{II} are the fracture energy components of Modes I and II, respectively; $G_{F\mathrm{I}}$ and $G_{F\mathrm{II}}$ are the critical fracture energies under pure Modes I and II loading, respectively.

The interfacial fracture energy, which is crucial in the analysis of the FRP-concrete bonded joint, represents the total external energy required to create, propagate and fully open a crack along the FRP-concrete interface. Finding the right value of the interfacial fracture energy of the analysed interface remains an open issue due to the number of parameters governing the local bond–slip behaviour as well as the bond strength of the FRP-concrete joint itself. These include the tensile, compressive, and shear strengths of concrete, the tensile strengths of the adhesive and the FRP strip, the moduli of elasticity of all components of the joint, as well as its main dimensions.

It is worth mentioning that, in the case of mixed-mode conditions, the Mode I (tensile) fracture energy of concrete-FRP joints can be approximated by the Mode I fracture energy of plain concrete, provided that debonding in the concrete-FRP bonded joint takes place within concrete. A second observation is that the Mode II (shear) fracture energy of both plain concrete and FRP-concrete joint appears to be an order of magnitude higher than that for Mode I [14].

3. Numerical analysis of the direct-shear test

The subject of this study is the simulation of a single direct-shear test on an FRP-to-concrete bonded joint, as presented in Fig. 1, where the main dimensions are shown. The applied constraints are intended to prevent the concrete prism from uplifting and shifting under loading. The FRP strip is bonded with an adhesive layer to the top surface of the concrete prism. Three lengths of joint – 10 cm, 15 cm, and 20 cm, and two types of adhesive layers with different stiffnesses were considered. Displacement-controlled loading was used by incrementing the displacement u at the end of the FRP strip (Fig. 1).

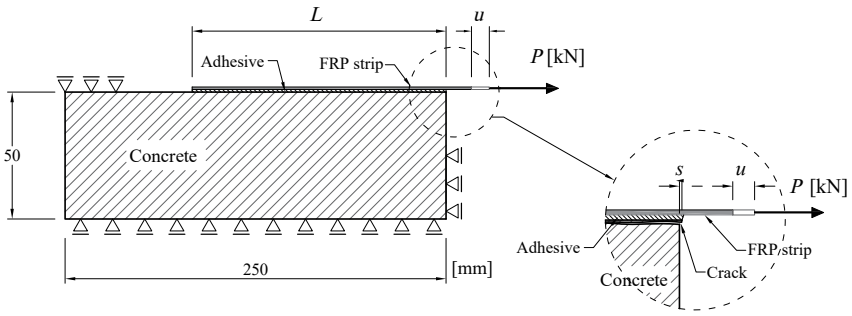

Fig. 1. Setup of the analysed direct-shear test.

The plots of reaction force P and slip s at the FRP-concrete interface were then obtained.

In the numerical analyses, the XFEM method implemented in Abaqus ver. 2024 code [15] was used. The failure mechanism definition includes damage initiation as well as damage evolution, which are based on a fracture mechanics approach and on the assumed bilinear traction-separation law for the FRP-concrete interface (Fig. 2). It was not necessary to predefine the crack initiation in the mesh layout for further propagation. This is one of the most convenient capabilities provided by the XFEM method.

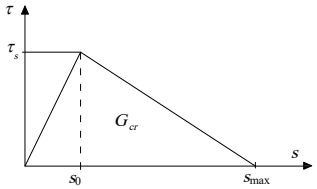

τ – shear bond stress
τ_s – shear bond strength
s – bond separation slip
s_0 – local slip at τ_s
s_{max} – maximum bond separation slip
G_{cr} – interfacial fracture energy (G_{cr}= G_{FII})

FIG. 2. Bilinear traction-separation law for the FRP-concrete interface.

When analysing the traction-separation law for the FRP-concrete interface, the area under the entire curve (Fig. 2) represents the interfacial fracture energy G_{cr}, which is equal to the value of the fracture energy G_{FII} for Mode II.

All parts of the numerical model are defined as elastic materials. The concrete prism, as well as the adhesive layer and FRP strip, are modelled using 4-node 2D plane strain elements (Fig. 3) of 1 mm × 1 mm dimensions. Although XFEM is often described as mesh-independent because cracks can propagate through elements without the mesh conforming to the crack geometry, it still requires a sufficiently fine mesh to obtain accurate results, especially near crack tips where stresses are singular. For this reason, a convergence study was performed by varying the element size. Analyses with different element sizes were performed, namely 1 mm × 1 mm, 1.5 mm × 1.5 mm, and 2 mm × 2 mm meshes. Finally, a mesh with an element size of 1 mm × 1 mm was used in all calculations,

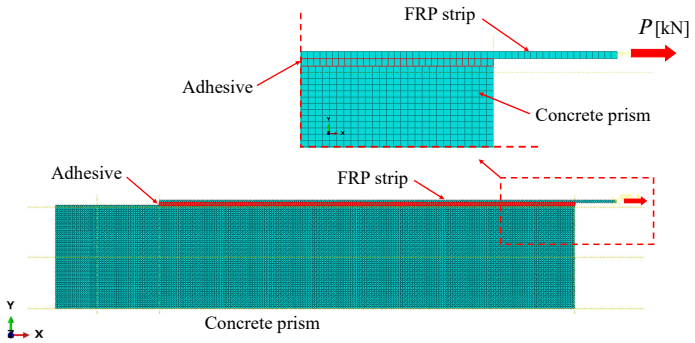

FIG. 3. 2D mesh of concrete prism with FRP strip.

for which the peak load did not change by more than 0.7 % compared to that obtained with the 1.5 mm × 1.5 mm mesh.

It was observed in laboratory tests [5] that the quasi-brittle behaviour of concrete influences the FRP debonding process. Fracture propagation during IC debonding starts within a thin concrete layer underlying the adhesive layer [5, 18, 30]. It was assumed that, in the case of the shear test for all tested bond lengths, delamination also starts within a thin concrete layer, beginning close to the loaded end of the FRP strip [16, 30]. For this reason, a one-element-thick layer of finite elements in the concrete part of the numerical model was given additional enrichment with additional degrees of freedom according to XFEM.

The material data used in the numerical analyses were taken from a previously performed research program concerning the flexural strengthening of simply supported RC beams using FRP strips [5]. For concrete, the modulus of elasticity and Poisson's ratio before cracking were determined as 29.98 GPa and 0.164, respectively. The concrete compressive cylinder strength was assumed as 44.40 MPa, while the tensile strength was determined as 3.467 MPa. The modulus of elasticity and Poisson's ratio of the FRP strips were taken as 158.95 GPa and 0.2, respectively. For the flexible adhesive, the modulus of elasticity and Poisson's ratio were equal to 7.10 GPa and 0.3, respectively. To check the influence of the stiffness of the adhesive layer on the behaviour of the entire joint, a case with a rigid adhesive with an elastic modulus 10 times higher than the stiffness modulus assumed for the flexible adhesive, was also considered [9].

The proper definition of the traction-separation law for the FRP-concrete interface is a key issue in delamination analysis by XFEM (Fig. 2). It mainly concerns the stress value τ_s, which is used to define the damage initiation criterion, as well as the interfacial fracture energy G_{cr}, which is equal to the value $G_{F\mathrm{II}}$ for the FRP-concrete joint. This value is, in turn, used in the definition of crack evolution. In our case of 2D analysis, in Eq. (2.1), two stress components, namely σ_n and τ_s, must be defined as the component normal to the potential cracked surface and as the shear component to the likely cracked surface, respectively. While the first component corresponds to the tensile strength of concrete, the second component cannot be determined directly. According to [8], the value of the shear strength τ_s depends on both the tensile strength of concrete as well as on the geometry of the FRP-concrete joint. Taking into account the width of the FRP strip and the width of the concrete prism, τ_s was calculated as 5.721 MPa [8].

Another important issue in delamination analysis is to assume correct and reliable values of fracture energy G_{Fi} parameters [14, 30]. While finding the fracture energy value $G_{F\mathrm{I}}$, which refers to fracture energy for Mode I (tensile) is rather straightforward, then finding the proper fracture energy value $G_{F\mathrm{II}}$ for Mode II (shear), which refers to the interface failure of the FRP-concrete joint,

is not easy. In this study, the value of $G_{F\mathrm{I}}$ is assumed as 0.090 kN/m as a function of both maximum aggregate size and the strength class of concrete [31]. The value of fracture energy for the FRP-concrete interface $G_{F\mathrm{II}}$ depends strongly on the geometry of a joint as well as on one of two basic strengths of concrete. According to [6, 8, 10] the value of fracture energy $G_{F\mathrm{II}}$ for Mode II is calculated as 0.694 kN/m as a function of tensile strength of concrete, but in accordance to [14] it could be also assumed as 1.524 kN/m as a function of compressive strength of concrete. There is a significant discrepancy between the two calculated values, which confirms the need for future laboratory verification of that interface fracture energy value. In the present numerical analyses to estimate the influence of different parameters on the behaviour of the FRP-concrete bonded joint, both above mentioned values of $G_{F\mathrm{II}}$ are used in definition of damage evolution law.

4. Numerical results

A series of numerical analyses was performed, and some general conclusions are drawn hereafter.

The influence of different values of the interfacial fracture energy $G_{F\mathrm{II}}$ on the strength of the FRP- concrete bonded joint was examined first. It was noted earlier that the value of this energy is crucial in modelling the FRP-concrete joint and it has a significant effect on its strength. The results of the study for a bond length equal to 20 cm are presented in Fig. 4. They are in good agreement with those proposed in [6], where, for considered fracture energies, the ultimate load capacity of the bonded joints were calculated as approximately 26 kN and 38 kN, respectively. It is worth noticing that, in the simplified analytical formula, the ultimate load does not depend on the bond length.

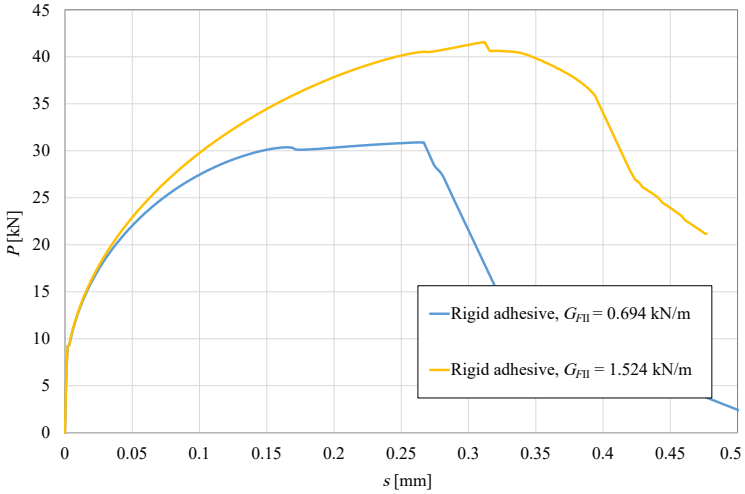

Fig. 4. Load-slip curves for a 20 cm joint for different values of interfacial fracture energy.

Most debonding models neglect the effect of adhesive stiffness. In reliable modelling, this effect should be taken into consideration because, as it was shown, for example, in [9], the adhesive stiffness may affect the ultimate bond capacity of the FRP-concrete interface. The results of the analyses for one bond length, for rigid and flexible adhesive, and for the two considered interfacial fracture energies are presented in Fig. 5. It is shown that the use of a rigid adhesive increases the bond strength of the FRP-concrete joint – the lower the value of interfacial fracture energy, the greater the increase of bond strength of the joint. It is also seen that a flexible adhesive shifts the bond capacity horizontally and makes the FRP-concrete interface more ductile.

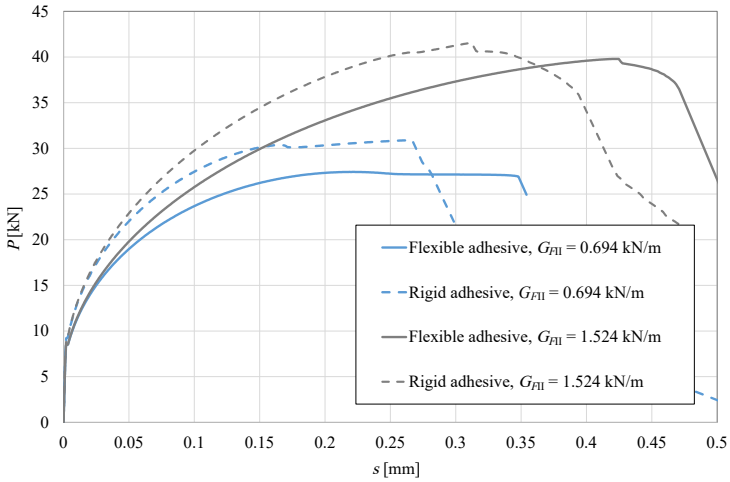

FIG. 5. Load-slip curves for a 20 cm joint for different types of adhesives and different values of interfacial fracture energy.

The effective bond length is defined as the length of the composite strip beyond which, there would be no increase in the force transferred between concrete and the FRP strip. So, a properly assumed effective length of the FRP strip is another key parameter in the modelling of such joints. This aspect is examined next in our study.

Analyses were performed for three different bonding lengths: 10 cm, 15 cm, and 20 cm. The results of these analyses are presented in Fig. 6, where it can be seen that the bond strength is higher for longer bond lengths.

To find out the value of the effective length of the FRP strips, the analysis of the axial strain ε_{11} along the joint between the strip and the concrete is carried out for different levels of loadings. In Fig. 7 and Fig. 8, the results of these analyses are shown, and the strain ε_{11} distributions along the strip are presented for two cases of joint lengths (10 cm and 20 cm). It can be noticed from Fig. 7b that the strain ε_{11} approaches zero at about $x = 3.5$ cm for a load close to the

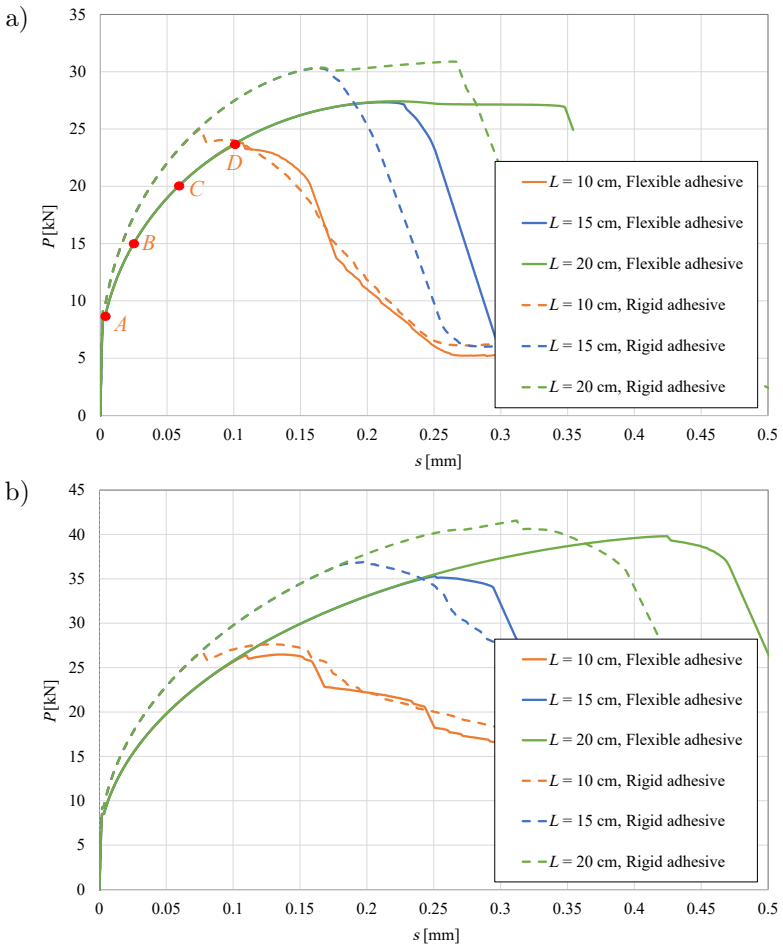

FIG. 6. Load-slip curves for different bond lengths and different types of adhesive layer: a) $G_{FII} = 0.694\,\text{kN/m}$, b) $G_{FII} = 1.524\,\text{kN/m}$.

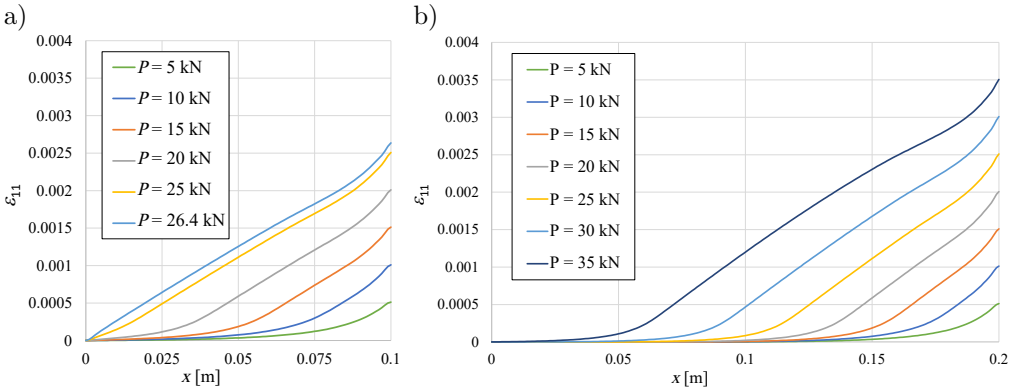

FIG. 7. Strain ε_{11} along the strips for flexible adhesive with $G_{FII} = 1.524\,\text{kN/m}$ and for different bond lengths: a) $L = 10\,\text{cm}$, b) $L = 20\,\text{cm}$.

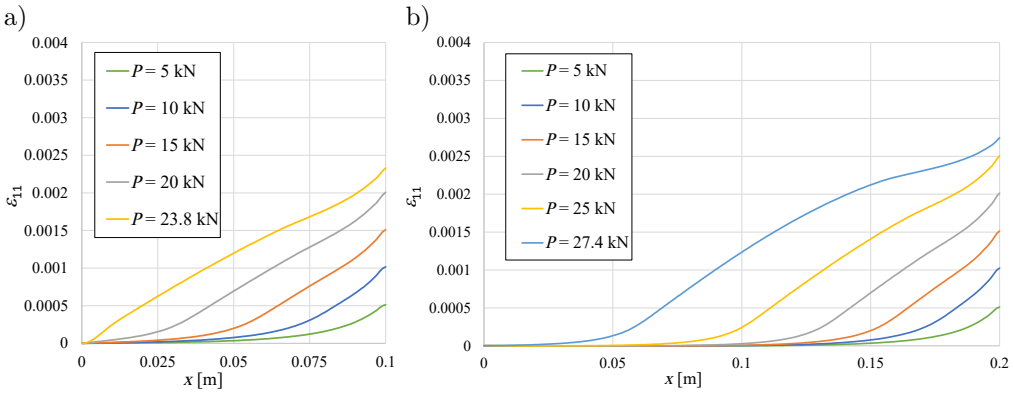

FIG. 8. Strain ε_{11} along the strips for flexible adhesive with $G_{F\mathrm{II}} = 0.694\,\mathrm{kN/m}$ and for different bond lengths: a) $L = 10\,\mathrm{cm}$, b) $L = 20\,\mathrm{cm}$.

ultimate value. This means that the effective bond length value is about 16.5 cm, which corresponds very well to that obtained in [31]. For the strip length equal to 10 cm, a similar trend does not occur, what is clearly seen in Fig. 7a. This confirms that a length of 10 cm turns out to be underestimated.

The strain paths show the higher strain ε_{11} levels and better utilization of the FRP strip for a strip length of 20 cm, regardless of the type of adhesive layer.

To illustrate crack progression during the shear test, contour plots of crack progression (scaled $\times 10$) for different load levels indicated in Fig. 6a are shown in Fig. 9, for the case of a flexible adhesive with $G_{F\mathrm{II}} = 0.694\,\mathrm{kN/m}$ and a bond length equal to 10 cm.

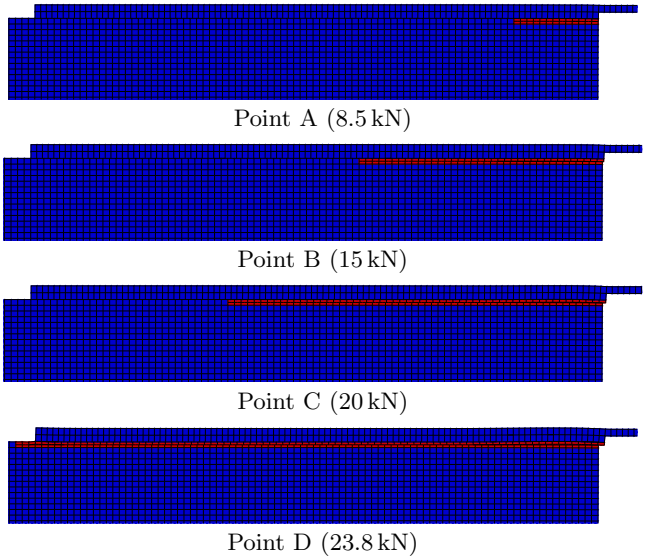

FIG. 9. Contour plots of crack progression (flexible adhesive; $G_{F\mathrm{II}} = 0.694\,\mathrm{kN/m}$; bond length 10 cm) for different load levels (Fig. 6a).

5. Final conclusions

This paper presented the major results of the study on the direct-shear test on the FRP-concrete bonded joints using the XFEM. The applied method successfully allowed to analyze the FRP-concrete joint, which is a highly discontinuous and nonlinear phenomenon that cannot be fully captured by standard FEM.

Based on the performed numerical analyses, it was found that a key issue in modelling is to adopt an appropriate interfacial fracture energy.

The effective bond length is another important parameter, as it not only determines the effectiveness of the joint but also affects its strength.

Consideration of the adhesive stiffness in modelling is important because it impacts the local bond-slip behaviour of the FRP-concrete interface and, subsequently, affects its load-carrying capacity.

The aforementioned parameters are the most important ones in governing the bond–slip behaviour as well as the bond strength of the FRP-concrete joints. These parameters will be the subject of planned laboratory tests to validate them.

Fundings

The work was financially supported by Poznan University of Technology, Institute of Civil Engineering (grant no. 0413/SBAD/6602).

Conflict of interests

The author declares that there are no known competing financial interests or personal relationships that could have influenced the work described in this paper.

Author's contribution

The author conceptualized the study, performed the analysis, wrote the original draft, and approved the final manuscript.

References

1. Teng J.G., Chen J.F., Smith S.T., Lam L., *FRP-Strengthened RC Structures*, John Wiley & Sons, Chichester, England, 2002.
2. Hammad M., Bahrami A., Khokhar S.A., Khushnood R.A., A state-of-the-art review on structural strengthening techniques with FRPs: Effectiveness, shortcomings, and future research directions, *Materials*, **17**(6): 1408, 2024, https://doi.org/10.3390/ma17061408.
3. Ortiz J.D., Khedmatgozar Dolati S.S., Malla P., Nanni A., Mehrabi A., FRP-reinforced/strengthened concrete: State-of-the-art review on durability and mechanical effects, *Materials*, **16**(5): 1990, 2023, https://doi.org/10.3390/ma16051990.

4. Kotynia R., *FRP Composites for Flexural Strengthening of Concrete Structures. Theory, Testing, Design*, Lodz University of Technology Press, Poland, 2019, https://doi.org/10.34658/9788372839961.

5. Jankowiak I., Analysis of RC beams strengthened by CFRP strips – Experimental and FEA study, *Archives of Civil and Mechanical Engineering*, **12**(3): 376–388, 2012, https://doi.org/10.1016/j.acme.2012.06.010.

6. Al-Saawani M.A., Al-Negheimish A.I., El-Sayed A.K., Alhozaimy A.M., Finite element modeling of debonding failures in FRP-strengthened concrete beams using cohesive zone model, *Polymers*, **14**(9): 1889, 2022, https://doi.org/10.3390/polym14091889.

7. Dai J., Ueda T., Sato Y., Unified analytical approaches for determining shear bond characteristics of FRP-concrete interfaces through pullout tests, *Journal of Advanced Concrete Technology*, **4**(1): 133–145, 2006, https://doi.org/10.3151/jact.4.133.

8. Lu X.Z., Teng J.G., Ye L.P., Jiang J.J., Bond–slip models for FRP sheets/plates bonded to concrete, *Engineering Structures*, **27**(6): 920–937, 2005, https://doi.org/10.1016/j.engstruct.2005.01.014.

9. Diab H.M., Farghal O.A., Bond strength and effective bond length of FRP sheets/plates bonded to concrete considering the type of adhesive layer, *Composites Part B: Engineering*, **58**: 618–624, 2014, https://doi.org/10.1016/j.compositesb.2013.10.075.

10. Chen J.F., Teng J.G., Anchorage strength models for FRP and steel plates bonded to concrete, *Journal of Structural Engineering*, **127**(7): 784–791, 2001, https://doi.org/10.1061/(ASCE)0733-9445(2001)127:7(784).

11. American Concrete Institute, *Guide for the design and construction of externally bonded FRP systems for strengthening concrete structures* (ACI 440.2R-08), USA, 2008.

12. FIB Bulletin 90, *Externally applied FRP reinforcement for concrete structures*, Technical report, Lausanne, Switzerland, 2019, https://doi.org/10.35789/fib.BULL.0090.

13. Cornetti P., Corrado M., De Lorenzis L., Carpinteri A., An analytical cohesive crack modeling approach to the edge debonding failure of FRP-plated beams, *International Journal of Solids and Structures*, **53**: 92–106, 2015, https://doi.org/10.1016/j.ijsolstr.2014.10.017.

14. Gunes O., Buyukozturk O., Karaca E., A fracture-based model for FRP debonding in strengthened beams, *Engineering Fracture Mechanics*, **76**(12): 1897–1909, 2009, https://doi.org/10.1016/j.engfracmech.2009.04.011.

15. Dassault Systemes, *Abaqus user's guide*, USA, 2024.

16. Benvenuti E., Vitarelli O., Tralli A., Delamination of FRP-reinforced concrete by means of an extended finite element formulation, *Composites Part B: Engineering*, **43**(8): 3258–3269, 2012, https://doi.org/10.1016/j.compositesb.2012.02.035.

17. Mohammadi T., *Failure mechanisms and key parameters of FRP debonding from cracked concrete beams*, Ph.D. Thesis, Marquette University, USA, 2014.

18. Jankowiak I., XFEM analysis of intermediate crack debonding of FRP strengthened RC beam, [in:] *Advances in Mechanics – Theoretical, Computational and Interdisciplinary Issues*, Kleiber M., Burczyński T., Wilde K., Górski J., Winkelmann K., Smakosz Ł. [Eds], pp. 235–239, CRC Press, London, 2016.

19. Mohammadi T., Wan B., Harries K., Intermediate crack debonding model of FRP-strengthened concrete beams using XFEM, SIMULIA Community Conference, Dassault Systèmes, Paris, 2013, https://doi.org/10.13140/RG.2.1.3597.2641.

20. Belytschko T., Black T., Elastic crack growth in finite elements with minimal remeshing, *International Journal for Numerical Methods in Engineering*, **45**(5): 601–620, 1999, https://doi.org/10.1002/(SICI)1097-0207(19990620)45:5<601::AID-NME598>3.0.CO;2-S.

21. Moës N., Dolbow J., Belytschko T., A finite element method for crack growth without remeshing, *International Journal for Numerical Methods in Engineering*, **46**(1): 131–150, 1999, https://doi.org/10.1002/(SICI)1097-0207(19990910)46:1<131::AID-NME726>3.0.CO;2-J.

22. Moës N., Belytschko T., Extended finite element method for cohesive crack growth, *Engineering Fracture Mechanics*, **69**(7): 813–833, 2002, https://doi.org/10.1016/S0013-7944(01)00128-X.

23. Tejchman J., Bobiński J., *Continuous and Discontinuous Modelling in Fracture in Concrete Using FEM*, Springer, Berlin, Heidelberg, 2013, https://doi.org/10.1007/978-3-642-28463-2.

24. Melenk J.M., Babuška I., The partition of unity finite element method: Basic theory and applications, *Computer Methods in Applied Mechanics and Engineering*, **139**(1–4): 289–314, 1996, https://doi.org/10.1016/S0045-7825(96)01087-0.

25. Sukumar N., Huang Z.Y., Prévost J.-H., Suo Z., Partition of unity enrichment for bimaterial interface cracks, *International Journal for Numerical Methods in Engineering*, **59**(8): 1075–1102, 2004, https://doi.org/10.1002/nme.902.

26. Golewski G.L., Golewski P., Sadowski T., Numerical modelling crack propagation under Mode II fracture in plain concretes containing siliceous fly-ash additive using XFEM method, *Computational Materials Science*, **62**: 75–78, 2012, https://doi.org/10.1016/j.commatsci.2012.05.009.

27. Watkins J., Fracture toughness test for soil-cement samples in mode II, *International Journal of Fracture*, **23**: R135–R138, 1983, https://doi.org/10.1007/BF00020700.

28. Rocha R.J.B., Campilho R.D.S.G., Evaluation of different modelling conditions in the cohesive zone analysis of single-lap bonded joints, *The Journal of Adhesion*, **94**(7): 562–582, 2018, https://doi.org/10.1080/00218464.2017.1307107.

29. Whitcomb J.D., *Analysis of instability-related growth of a through-width delamination*, NASA Technical Memorandum (TM), Report no. NASA-TM-86301, 1984.

30. Carloni C., Analyzing bond characteristics between composites and quasi-brittle substrates in the repair of bridges and other concrete structures, [in:] *Advanced Composites in Bridge Construction and Repair*, Kim Y.J. [Ed.], Woodhead Publishing, pp. 61–93, 2014, https://doi.org/10.1533/9780857097019.1.61.

31. CEB-FIP, *Model Code 1990. Design Code*, Comité Euro-International du Béton, Lausanne, Switzerland, 1993 (Republished 1998).

Received July 28, 2025; revised September 30, 2025; accepted November 1, 2025; available online December 12, 2025; version of record April 13, 2026; published issue XXXX.